

The Cartwheel ring under X-ray light

A. Wolter¹ and G. Trinchieri¹

¹INAF - Osservatorio Astronomico di Brera via Brera 28, 20121 Milano

Abstract. The Cartwheel, archetypical ring galaxy with strong star formation activity concentrated in a peculiar annular structure, has been imaged with the CHANDRA ACIS-S instrument. We present here preliminary results, that confirm the high luminosity detected earlier with the ROSAT HRI. Many bright isolated sources are visible in the star-forming ring. A diffuse component at luminosity of the order of 10^{40} cgs is also detected.

Key words. galaxies: individual: A0035-324=Cartwheel – galaxies: starburst – X-rays: galaxies

1. The Cartwheel

The Cartwheel (A0035-324) is a spectacular ring galaxy, located in a tight group at $z \sim 0.03$, of about 0.2 Mpc physical size. The ring-shaped galaxy formed after a head-on collision with a compact galaxy (one of the 4 members of the group): the gravitational rebound generates a transient density wave that propagates outward and forms the ring. When/if the gas swept by the density wave reaches a “critical” density in the ring a process of intense star formation is triggered (eg. Hernquist & Weil (1993)).

Optical observations have revealed the presence of exceptionally luminous HII regions, with an estimated supernova rate as high as 1 SN/yr (Fosbury & Hawarden (1977)). A recent starburst in the outer ring of the Cartwheel is confirmed by the evidences provided by the data at many wavelengths, in particular at H α where many

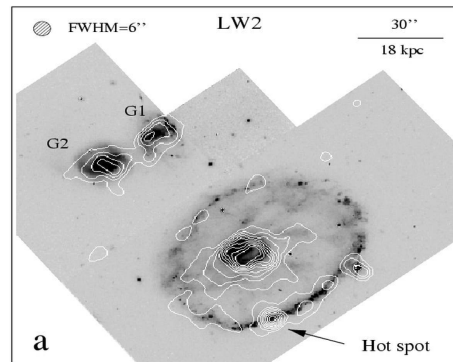


Fig. 1. The ISO contours at $7\mu\text{m}$ superposed on the HST image of the Cartwheel and its two close companions G1 and G2 (adapted from Charmandaris et al. (1999)).

HII regions are detected, and in the infrared, where ISO detects a hot spot in the south portion of the ring (Charmandaris et al. (1999), see Figure 1).

The first X-ray detection of the Cartwheel was obtained with the ROSAT

Send offprint requests to: A. Wolter
Correspondence to: anna@brera.mi.astro.it

HRI (Wolter et al. (1999)): the total flux of $F_x = 6.5 \times 10^{-14}$ cgs corresponds to an un-expectedly high luminosity of $L_x = 5.0 \times 10^{41}$ cgs, in the ROSAT band (we use $H_0 = 50 \text{ km s}^{-1} \text{ Mpc}^{-1}$, for a distance of 180 Mpc and a scale of 0.834 kpc/arcsec). We note that these numbers are virtually insensitive, in the ROSAT band, to the choice of spectral model that had to be assumed a priori due to the lack of spectral resolution of the HRI. The outer ring was clearly the sole site of emission, and the relatively high luminosity was interpreted as due to the enhanced level of star formation.

2. Chandra Images

We obtained in AO2 a CHANDRA ACIS-S 77 ksec exposure. (For a description of the CHANDRA mission see Weisskopf et al. (2000)). The CHANDRA image (see Figure 2) shows that the X-ray emission is extended and clumpy, mostly associated with the outer ring. The emission is stronger in the Southern quadrant, where the massive and luminous HII regions at large $H\alpha$ luminosities are found (Higdon (1995)). The ROSAT detection of the two nearby galaxies G1 and G2 is confirmed.

The smoothed X-ray data from the ACIS-S CHANDRA detector (see Figure 2) show that the many individual sources in the ring appear to be surrounded by a diffuse component. There is a slight indication of diffuse emission also in the center of the galaxy, but with no direct connection to the inner ring or the spokes. The nucleus is however clearly not detected, at a level of 10^{39} cgs. Giant HII regions and complex structures, typically coincident with peaks of $H\alpha$ emission, have been observed in actively star-forming objects like the interacting system “The Antennae” (NGC 4038/9; eg. Fabbiano et al. (1997)) as extremely bright X-ray sources, with intrinsic luminosities reaching several $\times 10^{40}$ cgs. To check this association in the Cartwheel, we have plotted the position of the HII knots as measured by Higdon (1995) onto the X-ray image in Figure 2. The positions of

the circles that mark the HII regions have been shifted by about 1” in RA and 0.5” in dec for better agreement with the X-ray peaks (well within the positional uncertainty of both the X-ray and the HII reference frame). A general trend in the locus of the X-ray and HII emission is evident. However, there is no one-to-one correspondence. The brightest individual source in the outer ring has a luminosity $L_X \sim 5 \times 10^{40}$ cgs in the ROSAT (0.2-2.4 keV) band, of the same order of those found in the Antennae.

3. Chandra spectra

From inspection of images in two different energy cuts we found that a diffuse emission is present, mostly in the soft band and most probably not confined to the ring only. We therefore decided to investigate the two components (isolated sources and diffuse emission) separately. We extracted a combined spectrum from all the individual sources, that we consider as point-like. The statistics is not such that a study of the individual profiles of the single sources will be significant, but in total we have more than 2500 net counts for the sum of the sources. Spectral data are binned so that each bin has a significance $\geq 2\sigma$.

The spectrum of the sum of the individual sources is shown in Figure 3 (*Top*). The data are fitted by a power law with $\Gamma = 1.4$ and $N_H = 9.1 \times 10^{20} \text{ cm}^{-2}$. The derived low energy absorption is higher than the galactic one, but consistent with the reddening observed in the HII regions. The contour plot of the uncertainties in spectral index and low energy absorption is shown in Figure 4. The photon index we obtain is in the range observed in other bright binaries in nearby galaxies when fitted with a simple power law model (eg. Humphrey et al. (2003)). The measured unabsorbed flux is 1.8×10^{-13} cgs (0.5-50 keV band) that corresponds to a Luminosity of 7.3×10^{41} (0.5-5.0 keV) cgs.

The spectrum shown in Figure 3 (*Bottom*) for the “extended” emission is

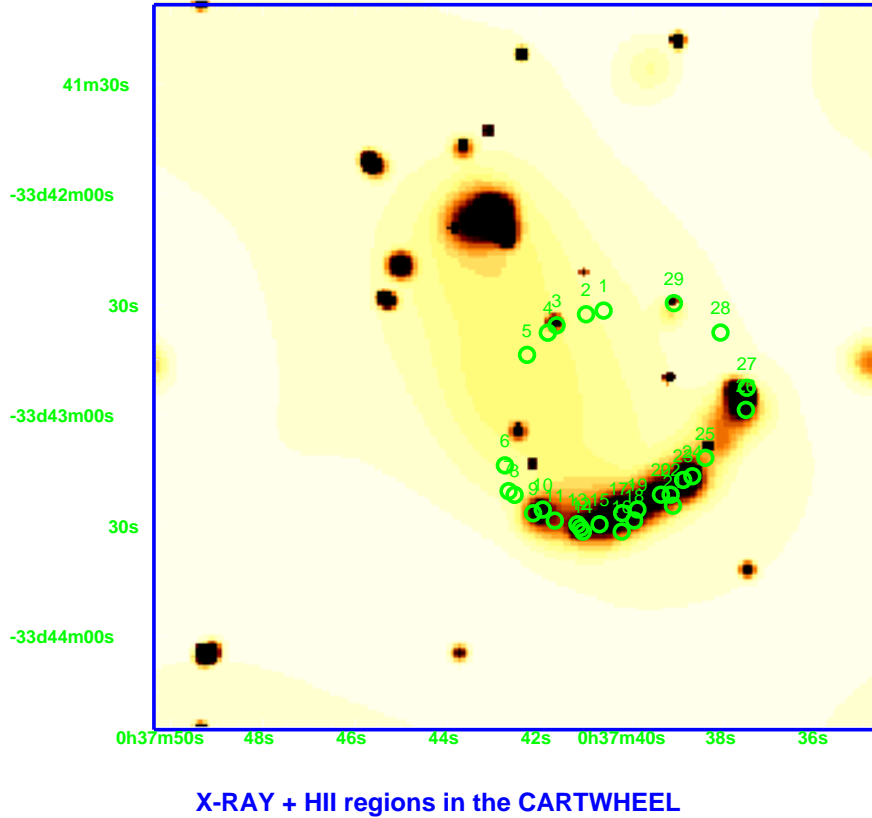


Fig. 2. The ACIS-S image, smoothed with *csmooth*. The circles mark the position of the HII knots measured by Higdon (1995).

derived from a region that includes virtually all of the Cartwheel extent, but excludes the point sources in the ring. While with only about 500 counts a successful detailed analysis is not guaranteed, we found that the spectrum can only be fitted by a complex model (at least two components, see Figure 3 *Center*). The best fit is a combination of a power law ($\Gamma=1.6$, $N_H=1.3 \times 10^{21} \text{ cm}^{-2}$ plus a plasma model (Raymond-Smith component with solar – fixed– abundance and $kT=0.3 \text{ keV}$).

The flux of the power law component, representing non-resolved binaries, is $F_x = 1.3 \times 10^{-14} \text{ cgs}$ (0.5–5.0 keV), about 10% of the resolved point source flux. The flux of the diffuse hot gas component is $F_x =$

$4. \times 10^{-15} \text{ cgs}$ (0.5–50 keV). It contributes mostly at 0.6–0.9 keV as expected from the temperature found. The total Luminosity of the gas is of the order of $1 - 2 \times 10^{40} \text{ cgs}$.

4. Conclusions

We have presented preliminary results from a CHANDRA observation of the Cartwheel. A number of isolated sources is present, coincident with the region of high star formation detected at other wavelengths. A diffuse gaseous component might permeate the entire system, but the detection is not on firm statistical grounds. The isolated sources have large X-ray luminosities, reaching a total of at least

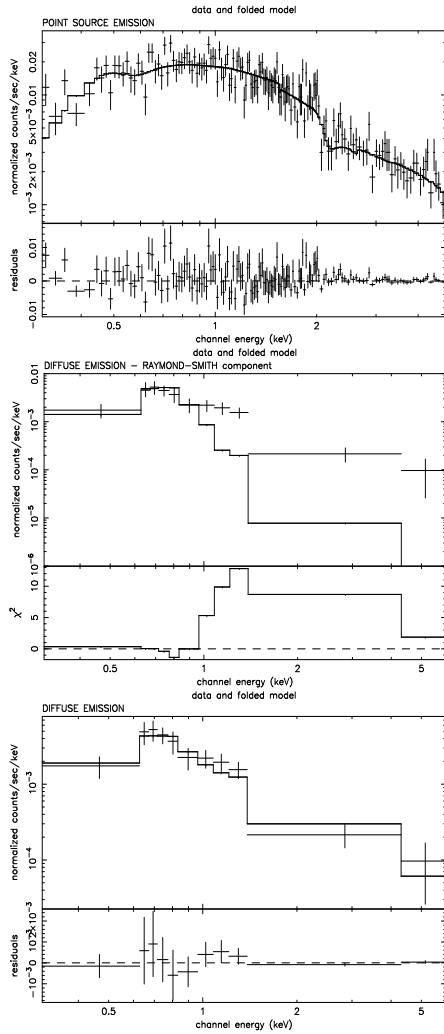


Fig. 3. *Top* ACIS spectrum of the combined individual unresolved sources. The solid line corresponds to a power law fit with $\Gamma = 1.4$ and $N_{\text{H}} = 9.1 \times 10^{20} \text{ cm}^{-2}$. *Center* ACIS spectrum of the diffuse component: even if the statistics is low, the spectrum can not be fitted by a single component. We show here the fit with a hot plasma component only: the hard tail is evident. The same kind of residuals is obtained by the fit with a power law component only. *Bottom* The same ACIS spectrum for the diffuse component: we show here the fit with a hot plasma component plus power law (see text for details).

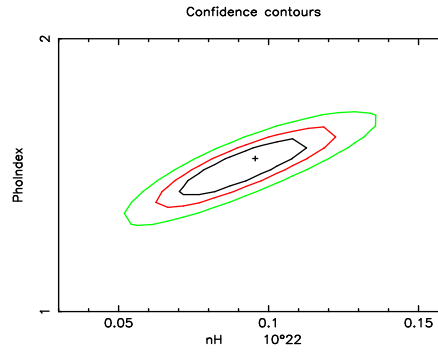


Fig. 4. Confidence contours of the two parameters Γ and N_{H} for the point-source spectrum.

$L_X = 7.3 \times 10^{41} \text{ cgs}$ in the 0.5-5.0 keV band. Future follow-up XMM data might help in deriving the spectra of the brightest individual sources thus confirming their identity, and firmly establish the presence and extent of the diffuse emission. Detailed analysis of the CHANDRA data will be presented in a forthcoming paper (Wolter et al. in preparation.)

Acknowledgements. This work has received partial financial support from the Italian Space Agency.

References

- Charmandaris V., Laurent O., Mirabel I.F., Gallais P., Sauvage M., Vigroux L., Cesarsky C., Appleton P.N. 1999, A&A 341, 69
 Fabbiano, G., Schweizer, F., and Mackie, G., 1997, ApJ, 478, 542
 Fosbury, R.A. and Hawarden, T.G., 1977, MNRAS 178, 473
 Hernquist L., and Weil M., 1993, MNRAS, 261, 804
 Higdon, J.L. 1995, ApJ 455, 524
 Humphrey P.J. et al. 2003, astro-ph/0305345
 Weisskopf, M., Tananbaum, H., Van Speybroek, L., & O'Dell, S., 2000 Proc. SPIE 4012 (astro-ph/0004127)
 Wolter A., Trinchieri G., Iovino A. 1999, A&A 342, 41